



Jilani, S. F., Aziz, A. K., Abbasi, Q. H. and Alomainy, A. (2018) Ka-band Flexible Koch Fractal Antenna with Defected Ground Structure for 5G Wearable and Conformal Applications. In: 2018 IEEE 29th Annual International Symposium on Personal, Indoor and Mobile Radio Communications (PIMRC), Bologna, Italy, 09-12 Sep 2018, pp. 361-364. ISBN 9781538660096.

There may be differences between this version and the published version. You are advised to consult the publisher's version if you wish to cite from it.

<http://eprints.gla.ac.uk/164515/>

Deposited on: 26 June 2018

Enlighten – Research publications by members of the University of Glasgow
<http://eprints.gla.ac.uk>

K_a-band Flexible Koch Fractal Antenna with Defected Ground Structure for 5G Wearable and Conformal Applications

Syeda Fizzah Jilani^{1,2}, Ahmed K. Aziz¹, Qammer H. Abbasi³ and Akram Alomainy¹

¹ School of Electronic Engineering and Computer Science, Queen Mary University of London, UK

² National University of Sciences and Technology, Islamabad, Pakistan

³ School of Engineering, University of Glasgow, Glasgow G12 8QQ, UK

{s.f.jilani, a.alomainy}@qmul.ac.uk

Abstract— This paper demonstrates a low profile, compact and conformal antenna design for 5th generation (5G) wireless devices. The antenna design incorporates two bandwidth-enhancement techniques of fractal geometry and defected ground structure (DGS). The Koch fractal radiating patch is developed with a DGS coupled coplanar waveguide (CPW) feeding. Highly precise fabrication is performed on a thin Polyethylene Terephthalate (PET) film using the additive manufacturing process of conductive ink-based inkjet printing. The results show that the antenna offers a bandwidth which covers K_a-band (26.5-40 GHz) and a peak realised gain of 9.7 dBi at 39.7 GHz. The integrated aperture in the ground improves the directivity by converging the radiation in the axis orthogonal to the antenna's plane. The proposed flexible antenna is well suited for integration in millimetre-wave (MMW) based wearable and conformal wireless devices.

Index Terms—5G; fractal; inkjet; Koch; PET.

I. INTRODUCTION

Upcoming 5G wireless architecture is anticipated to utilise the bandwidth of unused MMW spectrum to accomplish high capacity and data rates. Among the available high-frequency bands, 28- and 38-GHz are recommended by Federal Communication Commission (FCC), while the 26-GHz band is promoted by Office of Communications (Ofcom) to accommodate the demands of highly densified 5G architecture due to relatively lower propagation losses and atmospheric attenuations at such frequencies [1, 2]. The efficient and low-cost antenna is essential in this regard which provides high bandwidth to ensure high throughput, high gain to handle attenuations, preferably flexible and bendable to be deployed on both planar and non-planar surfaces, compact, low-cost and robust. The aggregation of such characteristics in a single antenna geometry is extremely challenging. A number of conformal devices and antennas have been proposed on substrates such as textile, polymer and polyesters films at MMW frequencies [3-5], yet there is still a need of further exploitation of K_a-band for 5G body-centric and wearable applications.

Fractal geometries have been widely used in antenna design, where the effective length and radiating area can be increased by insertion of fractals within a specified space [6]. For instance, in Koch fractals, the progression for the snowflake area is approximately 8/5 times the effective area of the initial triangle, and the edges/notches of fractals are responsible for improved bandwidth by generating additional resonances [7, 8]. Moreover, DGS geometries are considered as resonating defects or fractures intentionally created in the ground plane to interrupt the uniform current distribution and serve for either band-notching purpose or to incorporate added resonances [9, 10]. In addition, DGS symmetrical slots are inserted under or on either side of a feed line to directly couple with the feed of the antenna and thus controls the antenna's return loss characteristics [11].

Fabrication of flexible antennas at high frequency is critically demanding due to smaller feature size which requires high accuracy. Inkjet printing is an additive fabrication technique and considered as a suitable choice for antenna prototyping on thin films with a high level of accuracy as compared to other related processes such as, photolithography which requires much more complexity, or relatively less-precise screen printing fabrication. In this paper, the flexible antenna integrates second-order iteration of Koch fractals and a DGS-coupled feed line to achieve high bandwidth and high gain. These properties will enable the antenna to be a part of flexible wearable applications in upcoming 5G networks.

II. ANTENNA DESIGN AND FABRICATION

A. Antenna Design and Modelling

The antenna patch is designed based on traditional Koch fractal curves. The Koch curves are modelled by embedding two equilateral triangles back-to-back in a shape of a star, which increases the radiating area inside the same footprint. Mathematically, the design is initiated with an equilateral triangle and for the first iteration, each side of the triangle is divided into three equal sections, where the middle 1/3rd segment is being transformed by

another smaller equilateral triangle constructed by the side of $1/3$ unit. This results in a six-armed star. In this way, in the first iteration three $1/3$ unit sections are replaced by four segments of the same length and organised such that the end-points remain confined between the actual length of iteration zero. This method adjusts the angles of the extended equilateral triangle geometry and increases the actual area confined by the triangle within the same footprint. Furthermore, in the second iteration, the same procedure is repeated on each of the sides and the middle section is being replaced with smaller equilateral triangles. Mathematical modelling of the equilateral triangle at a resonant frequency of 32 GHz is done by using eq. (1)-eq. (3) [12]. However, the eq. (4) represents the number of sides in each iteration for the generation of Koch fractals and eq. (5) computes the length of each side after each iteration [13].

$$a_e = a \sqrt{1 + \frac{2h}{\pi\epsilon_r a} \left(\ln \frac{\pi a}{2h} + 1.7726 \right)} \quad (1)$$

$$f_{m,n,l} = \frac{2c}{3a_e(\epsilon_r)^{1/2}} (m^2 + mn + n^2) \quad (2)$$

$$f(1,0) = \frac{2c}{3a\sqrt{\epsilon_r}} \quad (3)$$

$$N_n = (3) (4)^n \quad (4)$$

$$L_n = (S) (1/3)^n \quad (5)$$

where a = patch length, ϵ_r = dielectric constant, and c = speed of light, m, n, l = mode-defining integers in eq. (2), f = resonant frequency, N = Number of sides, n = iteration number in eq. (4) and (5), L = Length of the side of fractal, S = length of a side of the equilateral triangle.

The initial length of the triangular patch is increased by Koch geometry and thus the fractal length is used to determine the resonant frequency of the antenna. The antenna is designed to resonate at 28-GHz band due to Koch geometry. The design and evaluation of the antenna is carried out in CST Microwave Studio. The advantages of DGS-coupled feeding network for bandwidth enhancement has been utilised in the proposed antenna [14]. The antenna is designed for single-sided printing, with the CPW feed-line coupled to a pair of symmetrical split-ring resonators (SRR) as a DGS. Also, an aperture for the placement of the Koch structure is incorporated in the ground plane. Parametric analysis is carried out for optimised placement and dimensions of the SRRs.

B. Antenna Fabrication

The antenna is fabricated on a flexible PET substrate ($\epsilon_r = 3.2$, $\tan\delta = 0.022$) of size $11.2 \times 12.5 \times 0.135$ mm³. Conductive silver nanoparticle ink is employed in a Dimatix Material printer (DMP-2831) calibrated with optimised settings of drop spacing, firing voltage, voltage waveform, jetting frequency and temperature. Post-printing curing and sintering are carried out to achieve a

conductivity of 0.6×10^7 S/m from a single printed layer. Heat sintering method is used and the printed prototype is placed in an oven set to a temperature of 150 °C for 40 minutes. K -connector is mounted on the feed-line of the antenna for measurements. The design parameters are shown in Fig. 1 (a), and corresponding dimensions are documented in Table 1.

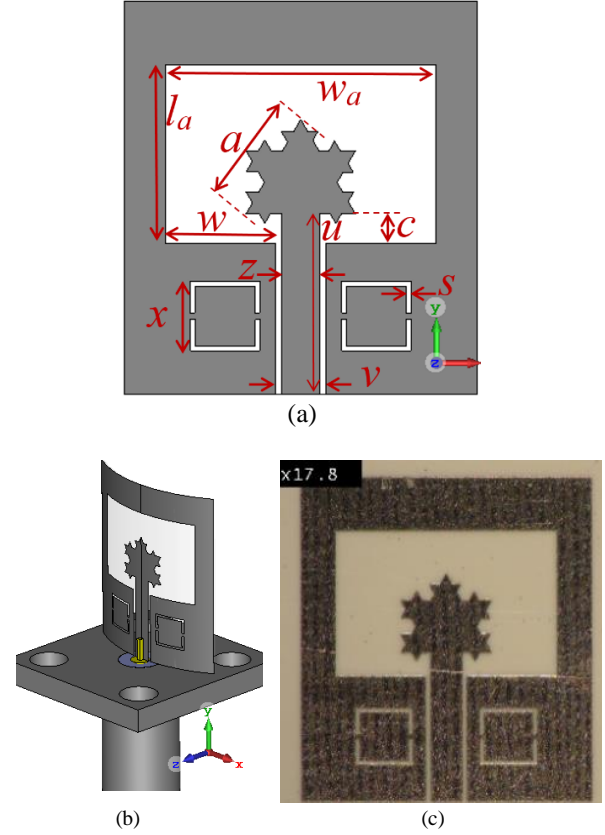


Fig. 1. Proposed Ka-band flexible antenna; (a) simulated antenna, (b) conformal model, (c) fabricated prototype by inkjet printing.

TABLE I. OPTIMISED DIMENSION OF THE PARAMETERS OF MMW KOCH FRACTAL ANTENNA.

Parameters	mm
Aperture length, l_a	5.7
Aperture width, w_a	8.6
Feed line length, u	5.75
Feed line width, z	1.2
CPW Gap for feed, v	1.6
Aperture side width, w	3.5
Length of patch side, a	3.46
Patch and aperture gap, c	0.95
Width of SRR slot, s	0.15
Length of square SRR, x	2.2

III. RESULTS AND DISCUSSION

The antenna performance is investigated based on the computational evaluations and parametric study of the simulated model in CST software as well as experimental testing of the inkjet-printed prototype, and the results are presented in this section.

A. Impedance Bandwidth

The antenna is mounted in both planar and conformal positions in the CST model. The radius of 10 mm is set for the curved cylindrical surface along which the antenna is bent for the conformal analysis. S_{11} plots of Fig. 2 depict that a bandwidth of 26–40 GHz is achieved with a close agreement between the simulated and measured results of the antenna. The simulated results in both configurations show similar S_{11} profile which depicts that the performance of the antenna is not affected by bending curvature. This justifies the claim of prospective implementation of the proposed fractal antenna in wearable and conformal applications.

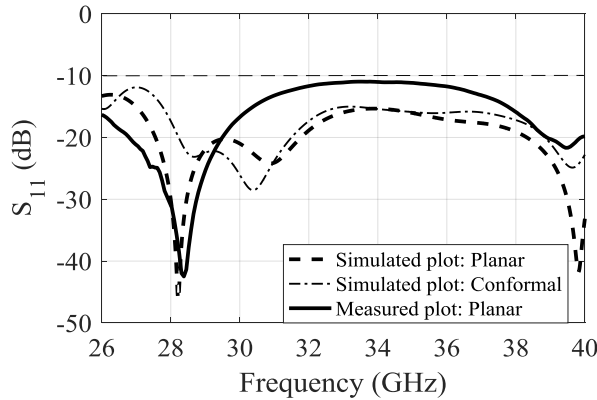


Fig. 2. Simulated and measured S_{11} plots of the proposed K_a -band flexible fractal antenna.

B. Radiation Pattern

The radiation characteristics of the proposed Koch fractal antenna are presented in Fig. 3. It is observed that the ground aperture surrounds the patch and minimises the radiation directivity along the antenna's plane and thus converges the beams on front and back of the antenna surface. However, the beams are not entirely orthogonal and tilted towards the end-fire direction due to the more metallic area of ground used for the SRR slots' placement inside the ground.

This tilted beam orientation can be clearly observed in E-plane cuts of Fig. 3 (a). However, the H-plane cuts in Fig. 3 (b) present the symmetrical distribution of radiation on front and back of the antenna. It is observed that bending of the proposed antenna on a curved surface has no significant effect on far-field radiation patterns of the antenna as the size of the antenna is much smaller than the extent of bending. Thus, the radiation response of

only planar configuration of the antenna is presented here.

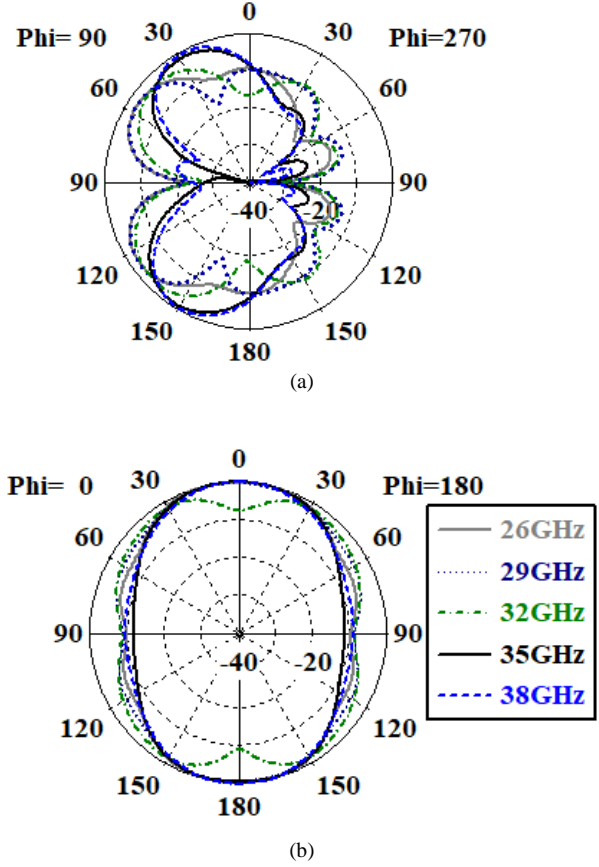


Fig. 3. Simulated radiation patterns of the proposed K_a -band flexible fractal antenna: (a) at $\phi = 90^\circ$; (b) at $\phi = 0^\circ$

C. Realised Gain and Efficiency

The high gain characteristics of the antenna is achieved by integration of several geometrical aspects for gain enhancement such as increased patch area due to fractals, radiating ground due to the SRR slots and beam convergence due to the designed aperture. Fig. 4 shows simulated results of realised gain and efficiency against the frequency of the proposed antenna over the complete K_a -band. The realised gain in both planar and conformal configurations represents almost similar profile over the operating bandwidth. The gain magnitude is lower in the frequency range between 26–28 GHz and rises gradually after 28 GHz. The gain is above 7 dBi from 28.5–40 GHz with a peak gain of 9.7 dBi is observed at 39.7 GHz.

The total efficiency of the proposed flexible antenna is approximately 80% or above in maximum part of the operating bandwidth. Though the efficiency falls below 80% before 28 GHz due to a lower gain magnitude at these frequencies, yet the efficiency in the frequency range from 28.6–40 GHz is above 80%, which shows efficient performance in maximum operating range.

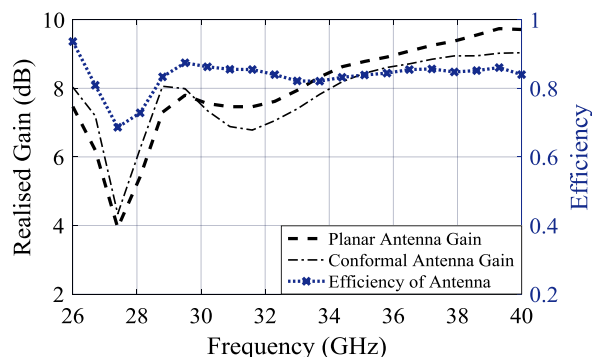


Fig. 4. Simulated peak realised gain and efficiency vs. frequency of K_a -band flexible fractal antenna.

IV. CONCLUSION

This paper has presented an inkjet-printed flexible K_a -band antenna aiming to achieve desired features of high bandwidth, conformity, cost-effectiveness and high-gain characteristics for future 5G networks. The antenna geometry integrates the benefits of Koch curves and DGS for incorporating additional resonant bands, merged to contribute a high bandwidth and high gain due to the increased effective radiating area within the same footprint. The antenna has been fabricated by the inkjet printing process on a PET substrate to attain the desired flexibility. The antenna offers bandwidth of complete K_a -band (26.5–40 GHz) with the efficiency of above 80%. A steady increase in gain profile with respect to frequency is observed with the peak gain of 9.7 dBi at 39.7 GHz. The proposed antenna is a potential contribution to the flexible wireless devices due to its efficient performance and conformity.

REFERENCES

[1] A. Gupta and R. K. Jha, "A survey of 5G network: architecture and emerging technologies," *IEEE Access*, vol. 3, pp. 1206–1232, 2015.

[2] W. Hong, K. H. Baek and S. Ko, "Millimeter-wave 5G antennas for smartphones: Overview and experimental demonstration," *IEEE Trans. Antennas Propag.*, vol. 65, no. 12, pp. 6250–6261, 2017.

[3] S. F. Jilani and A. Alomainy, "Planar millimeter-wave antenna on low-cost flexible PET substrate for 5G applications," *10th European Conf. Antennas Propag. (EuCAP)*, 2016, pp. 1–3.

[4] M. Ur-Rehman *et al.*, "A low profile antenna for millimeter-wave body-centric applications," *IEEE Trans. Antennas Propag.*, vol. 65, no. 12, pp. 6329–6337, Dec. 2017.

[5] N. Chahat *et al.*, "60-GHz textile antenna array for body-centric communications," *IEEE Trans. Antennas Propag.*, vol. 61, no. 4, pp. 1816–1824, Apr. 2013.

[6] S. F. Jilani, H. Ur-Rahman and M. N. Iqbal, "Novel star-shaped fractal design of rectangular patch antenna for improved gain and bandwidth," *IEEE Int. Symp. Antennas Propag. Soc. (APSURSI)*, 2013, pp. 1486–1487.

[7] S. Tripathi, A. Mohan and S. Yadav, "Hexagonal fractal ultra-wideband antenna using Koch geometry with bandwidth enhancement," *IET Microwaves, Antennas Propag.*, vol. 8, no. 15, pp. 1445–1450, 2014.

[8] Y. K. Choukiker and S. K. Behera, "Wideband frequency reconfigurable Koch snowflake fractal antenna," *IET Microwaves, Antennas Propag.*, vol. 11, no. 2, pp. 203–208, 2017.

[9] G. Breed, "An introduction to defected ground structures in microstrip circuits," *High Frequency Electronics*, 2008.

[10] J. Pei *et al.*, "Miniaturized triple-band antenna with a defected ground plane for WLAN/WiMAX applications," *IEEE Antennas Wireless Propag. Lett.*, vol. 10, pp. 298–301, 2011.

[11] L. H. Weng *et al.*, "An overview on defected ground structure," *Progress In Electromagnetics Research B*, vol. 7, pp. 173–189, 2008.

[12] R. Garg, S. A. Long, "An improved formula for the resonant frequencies of triangular microstrip patch antenna," *IEEE Trans. Antennas Propag.*, vol. 36, no. 4, pp. 570, Apr. 1988.

[13] M. T. Yassen *et al.*, "A compact dual-band slot antenna based on Koch fractal snowflake annular ring," *Progress In Electromagnetics Research Symp. - Spring (PIERS)*, 2017, pp. 670–674.

[14] M. T. Hafeez and S. F. Jilani, "Novel millimeter-wave flexible antenna for RF energy harvesting," *IEEE Int. Symp. Antennas Propag. & USNC/URSI National Radio Science Meeting*, 2017, pp. 2497–2498.